Non-coding RNA Research 9 (2024) 153–164

Contents lists available at ScienceDirect

Non-coding RNA Research

journal homepage: www.keaipublishing.com/en/journals/non-coding-rna-research

Original Research Article

Circ_ST6GAL1-mediated competing endogenous RNA network regulates TGF-β1-stimulated matrix Metalloproteinase-13 expression via Runx2 acetylation in osteoblasts

I. Saranya [a], R.L. Akshaya [a], K. Gomathi [a], R. Mohanapriya [a], Z. He [b], N.C. Partridge [b], N. Selvamurugan [a,*]

[a] Biotechnology, School of Bioengineering, SRMIST, Kattankulathur, India
[b] Molecular Pathobiology, New York University College of Dentistry, New York, USA

ARTICLE INFO

Keywords:
TGF-β1
Runx2
p300
Noncoding RNAs
microRNA
Circular RNA

ABSTRACT

Transforming growth factor-beta1 (TGF-β1) stimulates matrix metalloproteinase-13 (*MMP-13*, a bone-remodeling gene) expression, and this effect requires p300-mediated Runx2 (Runt-related transcription factor 2) acetylation in osteoblasts. p300 and Runx2 are transcriptional coactivator and bone transcription factor, respectively, which play key roles in the regulation of bone-remodeling genes. Non-coding ribonucleic acids (ncRNAs), such as long ncRNAs (lncRNAs) and microRNAs (miRNAs), have been linked to both physiological and pathological bone states. In this study, we proposed that TGF-β1-mediated stimulation of MMP-13 expression is due to the downregulation of p300 targeting miRNAs in osteoblasts. We identified miR-130b-5p as one of the miRNAs downregulated by TGF-β1 in osteoblasts. Forced expression of miR-130b-5p decreased p300 expression, Runx2 acetylation, and MMP-13 expression in these cells. Furthermore, TGF-β1 upregulated circ_ST6GAL1, (a circular lncRNA) in osteoblasts; circRNA directly targeted miR-130b-5p. Antisense-mediated knockdown of circ_ST6GAL1 restored the function of miR-130b-5p, resulting in downregulation of p300, Runx2, and MMP-13 in these cells. Hence, our results suggest that TGF-β1 influences circ_ST6GAL1 to sponge and degrade miR-130b-5p, thereby promoting p300-mediated Runx2 acetylation for MMP-13 expression in osteoblasts. Thus, the circ_ST6GAL1/miR-130b-5p/p300 axis has potential significance in the treatment of bone and bone-related disorders.

1. Introduction

The bone is a rigid organ with several functions; it regulates hematopoiesis, facilitates movement, and protects internal organs. It is highly dynamic and undergoes continuous remodeling (bone resorption and formation) throughout life. To maintain bone homeostasis, the balance between bone resorption and formation must be maintained [1]. Bone remodeling involves five steps (activation, resorption, reversal, formation, and mineralization [2,3] and requires several growth factors, hormones, and cytokines to regulate associated signaling cascades [4,5]. Transforming growth factor-beta (TGF-β) is a crucial cytokine in the bone [6]. Three distinct TGF-β isoforms are produced by mammals (TGF-β1, -2, and 3), with TGF-β1 receiving the most attention from scientists. TGF-β1 is highly abundant in the bone and plays a crucial role in bone remodeling by acting on osteoblasts (bone-forming cells) [7]. Matrix metalloproteinase-13 (MMP-13) is a collagenase responsible for degrading extracellular matrix (ECM) components, and defective MMP-13 expression causes skeletal dysplasia [8].

Studies have suggested that TGF-β1 and MMP-13 serve as coupling factors for bone formation and resorption. TGF-β1 induces MMP-13 expression in bone-forming cells by regulating Runt-related transcription factor 2 (Runx2, a bone transcription factor), Smad (suppressor of mothers against decapentaplegic), and ERK (extracellular signal-regulated kinase) signaling pathways [9–11]. Runx2 expression remains essential during the early stages of osteoblast differentiation, and defects in the expression of Runx2 can lead to cleidocranial dysplasia (CCD) [12–14]. An *in vivo* study in Runx2-null mice reported neither endochondral nor intramembranous bone formation, indicating its critical role in osteogenesis [15]. Previous findings have suggested that in the presence of TGF-β1, Runx2 is phosphorylated and then acetylated,

* Corresponding author. Biotechnology Department, School of Bioengineering, SRM Institute of Science and Technology, Kattankulathur, Tamil Nadu, India.
E-mail address: selvamun@srmist.edu.in (N. Selvamurugan).

https://doi.org/10.1016/j.ncrna.2023.11.002
Received 14 August 2023; Received in revised form 31 October 2023; Accepted 7 November 2023
Available online 10 November 2023

increasing its transcriptional activity with no change in its protein expression in osteoblasts [9–11,16,17]. Furthermore, p300, a transcriptional cofactor with histone acetyltransferase (HAT) activity, was found to acetylate Runx2 and influence its activity upon TGF-β1 treatment for MMP-13 expression in osteoblasts [17,18].

Non-coding RNAs (ncRNAs) have been implicated in controlling bone metabolism in both healthy and pathological circumstances, according to recent investigations [19,20]. ncRNAs, including short ncRNAs such as microRNAs (miRNAs), long ncRNAs (lncRNAs), such as linear RNAs (linRNAs), circular RNAs (circRNAs), serve as critical regulators of endogenous gene expression. Nearly all recognized biological processes, such as differentiation, cell growth, and proliferation, as well as development and metabolism, depend on miRNAs with an average length of 21–23 bases [21]. These tiny translational inhibitors complement the target mRNA and facilitate translational inhibition or degradation [22,23]. Multiple miRNAs act as important regulators of bone formation and resorption genes, including essential transcription factors and cofactors required for the complex process of bone remodeling.

CircRNAs are a unique type of lncRNAs that are generated by back splicing and have multiple roles, such as protein translation regulation, miRNA and protein sponging, and gene transcription regulation [24]. Among the various roles listed, sponging of miRNAs by circRNAs has been widely studied and commonly discussed in the literature. CircRNAs function as competitive endogenous RNAs (ceRNAs) and possess the miRNA-responsive element (MRE) that interacts with their target miRNAs, thereby controlling the expression of downstream mRNAs under both homeostasis and pathology [25]. We previously showed that TGF-β1 stimulates MMP-13 expression, and this effect requires p300-mediated Runx2 acetylation in osteoblasts [9,16]. In this study, we identified the molecular pathway that, in osteoblasts, regulates Runx2 acetylation through the circRNA/miRNA/p300 axis to stimulate MMP-13 expression in response to TGF-β1. According to our findings, TGF-β1 increases circ ST6GAL1, which functions as a ceRNA and scavenges miR-130b-5p. This enhances Runx2 acetylation by p300 and MMP-13 production in osteoblasts.

2. Materials and methods

2.1. Cell culture

In DMEM (Dulbecco's Modified Eagle Medium; Lonza, Italy), 10 % FBS (Fetal Bovine Serum; Gibco, USA), rat osteoblastic cells (UMR-106-01; NCCS, Pune) were maintained. Human bone marrow stromal cells (HS-5; ATCC, USA) or primary osteoblasts isolated from rat bone marrow (Isolation procedure was approved by the Animal ethical committee, University of Madras, India) were cultured in DMEM containing 10 % FBS, 10 nM β-glycerophosphate and 50 μM ascorbic acid [26]. The antibiotics used were streptomycin-amphotericin B/penicillin and streptomycin. They were maintained at 37°C in a humidified 5 % CO_2 incubator. The cells were treated with TGF-β1 (R&D Systems, USA; 5 ng/ml) at various time points after being incubated with 0.1 % FBS/DMEM to serum-starve the cells once they had reached 90 % confluence.

2.2. In-silico analysis

The p300 3′-untranslated region (UTR) sequence was procured using the Ensembl biomart interface (http://asia.ensembl.org/index.html), and miRBase (http://www.mirbase.org/) provided the available list of rat and human miRNA sequences. miRNAs putatively targeting the 3′-UTR of p300 were predicted using miRmap (https://mirmap.ezlab.org/), StarMiR (https://sfold.wadsworth.org/cgi-bin/starmirtest2.pl), and miRDB (http://mirdb.org/). Venny 2.1.0 (https://bioinfogp.cnb.csic.es/tools/venny/) was used to shortlist common miRNAs predicted by the three databases (Supplementary Fig. 1). TarBase (https://carolina.imis.athena-innovation.gr/diana_tools/web/index.php?r=tarbasev8%2Findex) and manual web searches were used to identify unvalidated miRNAs, which were further analyzed experimentally (Supplementary Table 1). CircRNA and miRNA interactions were predicted using circ2GO (https://circ2go.dkfz.de/. The workflow used to identify circRNAs is shown in Supplementary Fig. 2. Based on the *in-silico* analysis, we shortlisted 13 circRNAs. Antisense oligonucleotides (ASOs) for circ_ST6GAL1 were custom-designed and procured from Eurofins Genomics, USA (Supplementary Table 2).

2.3. Reverse transcriptase quantitative PCR (RT-qPCR)

Total RNA isolation was done using RNAisoplus reagent according to the manufacturer's recommendations. The extracted RNA was quantified and converted to cDNA using an iScript cDNA kit, and qPCR was carried out for precursor miRNAs and circRNAs with U6 and RPL13AB as the normalization genes, respectively, using the Applied Biosystems Quant Studio 3 instrument (Thermo Fisher Scientific, USA). Mature miRNA expression was achieved using the MiCury LNA kit, whereas U6 was employed as the endogenous control in qPCR. The relative expression of circRNAs, precursors, and mature miRNAs was determined using the ΔΔCt technique. Primers used in the precursor miRNA and circRNA analyses are listed in Supplementary Table 3.

2.4. Transient transfection

Using X-treme Gene transfection reagent (Roche, Basel, Switzerland), UMR-106-01 cells (70–80 % confluence) were transfected with negative control miRNA (nc-miRNA), miR-130b-5p mimic, or ASO for circ_ST6GAL1 at 50 nM concentration in accordance with the company's protocol (Qiagen, Germany). 24 h post-transfection, the cells were then subjected to TGF-β1 treatment for 2, 8, or 24 h. Protein samples were utilized for immunoprecipitation and western blotting, while extracted total RNA was used for RT-qPCR testing.

2.5. Immunoprecipitation and western blotting

Protein lysates were collected from transfected samples and immunoprecipitation was performed as described earlier [11,16,17]. Western blot analysis was carried out on whole-cell lysates [11,17] using 1x radioimmunoprecipitation assay (RIPA) buffer including protease and phosphatase inhibitors. The blots were stripped and probed. Antibodies against p300 (Upstate Biotechnology; Cat # 05–257), MMP-13 (Proteintech; Cat # 18165-1-AP), acetyl-lysine (Cell Signaling Technology; Cat # 9441S), Runx2 (Santa Cruz Biotechnology; Cat # SC-390351), and α-tubulin (Santa Cruz Biotechnology; Cat # SC-5286) were used for probing. α-Tubulin was employed as an endogenous control.

2.6. Luciferase reporter assay

The luciferase reporter experiment was carried out as previously described [27,28] using an expression vector (pmirGLO-dual-luciferase miRNA target) obtained from Promega, WI, USA. Supplementary Table 4 displays synthetic antisense and sense oligonucleotides for the 3′-UTR of p300 and circ_ST6GAL1 in both their wild-type (Wt) and mutant (Mut) forms. The ratio of firefly activity to Renilla luciferase activity was used to calculate the relative luciferase activity. For normalization, the activity of Renilla luciferase activity was employed.

2.7. Statistical analysis

All quantitative data were gathered. One-way ANOVA was used to verify significant differences at various levels ($p < 0.001$, 0.01, and 0.05).

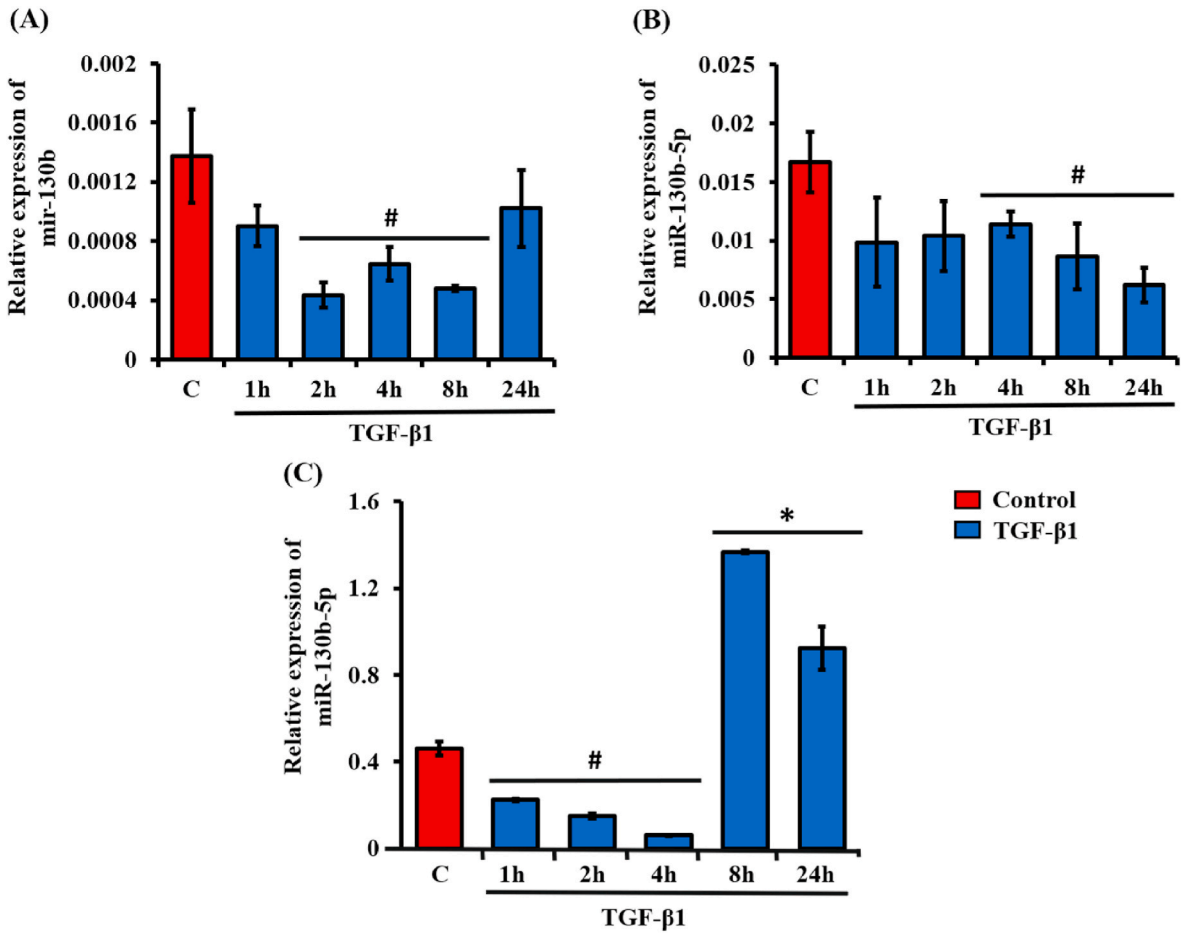

Fig. 1. TGF-β1 treatment downregulated miR-130b-5p expression in osteoblastic cells. For 1, 2, 4, 8, and 24 h, cells were exposed to control or TGF-β1 (5 ng/ml)-containing media. Total RNA was isolated, and cDNA synthesis and qPCR testing were carried out. **(A)** Relative expression of mir-130b in UMR-106-01 cells ($n = 3$). **(B)** Relative expression of miR-130b-5p in UMR-106-01 cells. **(C)** Relative expression of miR-130b-5p in HS-5 cells. U6 was served as the control for internal normalization. A significant increase over the corresponding control is indicated by an asterisk (*; $p \leq 0.05$). # Denotes a substantial reduction in comparison to the relevant control ($p \leq 0.05$).

3. Results

3.1. Predicting the list of miRNAs that may target the 3′UTR of p300 using bioinformatic analysis

The 3′ UTRs of p300 may be targeted by human and rat miRNAs, according to research done using bioinformatics methods (Supplementary Fig. 1). miRNA speculation tools, such as miRDB, STarMir Sfold, and miRmap provided a list of human and rat miRNAs that putatively targeted p300. Using Venny 2.1.0 software, we compared the rat miRNAs predicted by these three databases (mentioned as Ra All) with the miRNAs commonly predicted by three databases (miRDB, miRmap, and STarMir Sfold) for humans. Using Venny 2.1.0 software, nine miRNAs were found to putatively target p300 (Supplementary Fig. 1). The miRNAs validated in bone remodeling were eliminated from the common miRNA list using a manual web search and TarBase v7.0. Based on these results, we found a unique list of four miRNAs for p300, which have not been validated and were chosen for further analysis (Supplementary Table 1).

3.2. Downregulation of miR-130b-5p upon TGF-β1 treatment in osteoblasts

To confirm the presence and expression of the predicted miRNAs (Supplementary Fig. 1), we first determined the expression of four miRNAs (miR-551b, miR-186, miR-130b, and miR-339) at their precursor expression in rat osteoblasts by RT-qPCR analysis. We found a mixed pattern of upregulation and downregulation of miRNA expression at various TGF-β1 treatment periods, compared to the control. Among these four miRNAs, TGF-β1 treatment at 2, 4, and 8 h significantly reduced mir-130b expression in UMR-106-01 cells relative to the control (Fig. 1A). Since the other three miRNAs showed upregulation and downregulation of their expression by TGF-β1 treatment in these cells (data not shown), we selected mir-130b for further study. Next, we determined its expression at maturity. The results showed a significant downregulation of miR-130b-5p at 4, 8, and 24 h of TGF-β1 treatment, compared to that in the control in UMR-106-01 cells (Fig. 1B). In addition, we examined miR-130b-5p expression in osteoblasts derived from human bone marrow cells (HS-5). We found a significant downregulation of miR-130b-5p expression in HS-5 cells at 1, 2, and 4 h after TGF-β1 treatment compared to its control, which was consistent with the outcomes shown with UMR-106-01 (Fig. 1C).

3.3. Overexpression of miR-130b-5p decreased Runx2 acetylation in rat osteoblasts

Since we observed decreased expression of miR-130b-5p in osteoblasts treated with TGF-β1 (Fig. 1), we next determined its functional importance by its overexpression. We initially determined the transfection efficiency of miR-130b-5p in rat osteoblasts using RT-qPCR. There was a substantial upregulation in the endogenous expression of miR-130b-5p upon mimic transfection compared with that in the

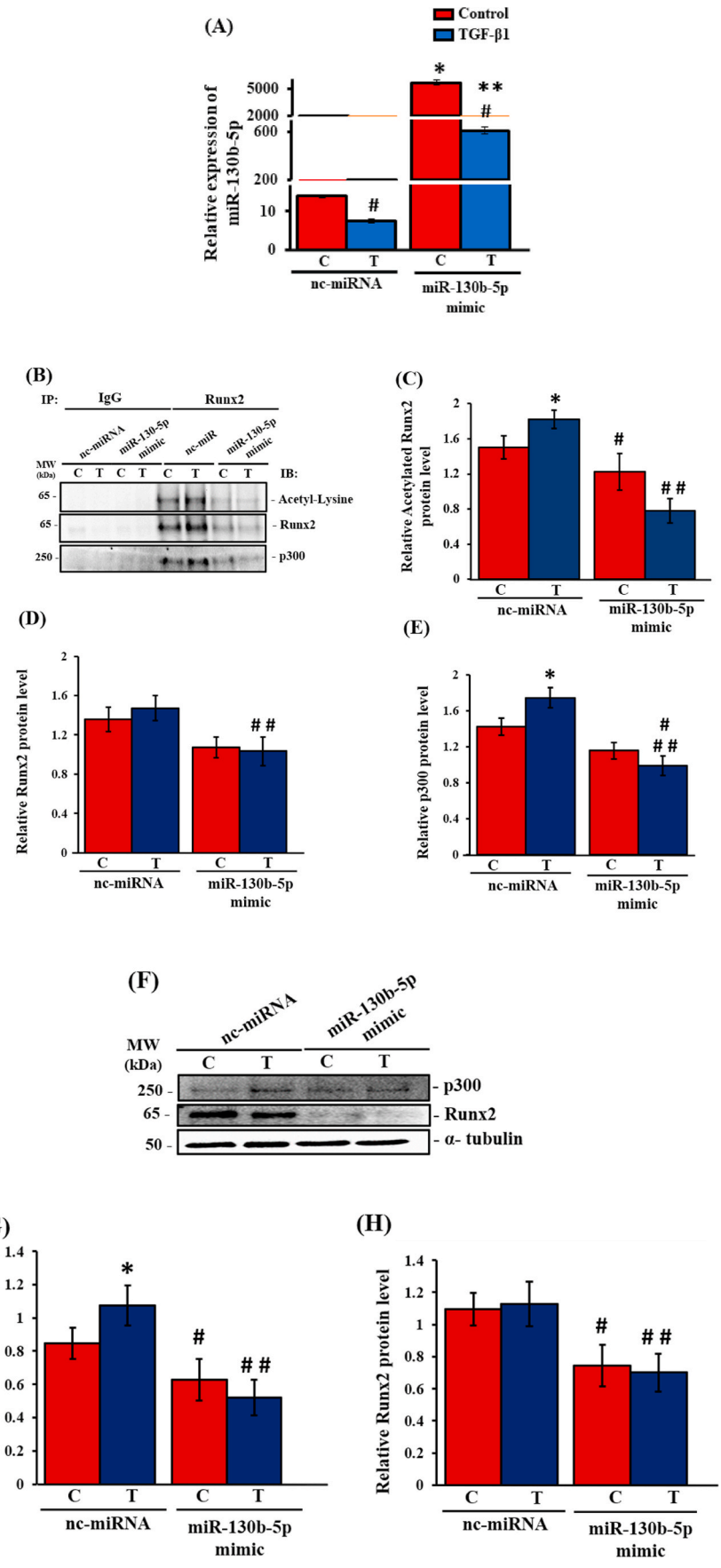

(caption on next page)

Fig. 2. In rat osteoblastic cells, overexpression of miR-130b-5p reduced Runx2 acetylation and p300 protein expression in response to TGF-β1. After transiently transfecting nc-miRNA or a miR-130b-5p mimic into UMR-106-01 cells for 24 h, TGF-β1 treatment was given for 2 h. Total cellular RNA as well as whole-cell lysates were collected. **(A)** Total RNA was used for cDNA synthesis, followed by qPCR analysis using the primers for miR-130b-5p. For normalization, U6 was employed as an internal control. * Denotes a substantial increase, compared to the control under nc-miRNA transfection, ($p < 0.01$); # Denotes a substantial decrease comparing in the corresponding control ($p < 0.01$); A significant improvement over the TGF-β1 treatment under nc-miRNA transfection is indicated using the symbol ** ($p < 0.0001$). **(B)** Immunoprecipitation (IP) of whole-cell lysates with Runx2 antibody or IgG was followed by immunoblot (IB) analysis with the anti-acetyl-lysine, anti-Runx2, and anti-p300 antibodies. A representative IP and IB blot is shown. After normalization with IgG, quantification of proteins was carried out using ImageJ software. Expression levels of **(C)** acetylated Runx2, **(D)** Runx2, and **(E)** p300 proteins ($n = 3$). **(F)** An aliquot of prepared whole-cell lysates was directly applied to Western blot analysis using p300, Runx2, or α-tubulin antibodies. A representative Western blot is shown. ImageJ software was used to quantify proteins after normalizing with α-tubulin. Expression levels of **(G)** p300 and **(H)** Runx2 proteins ($n = 4$). * Denotes a substantial increase over the corresponding control ($p < 0.01$); # Denotes a significant decrease compared to respective nc-miRNA transfection ($p < 0.01$); ## Denotes a significant decrease compared to that in the respective TGF-β1 treatment condition under nc-miRNA transfection ($p < 0.01$).

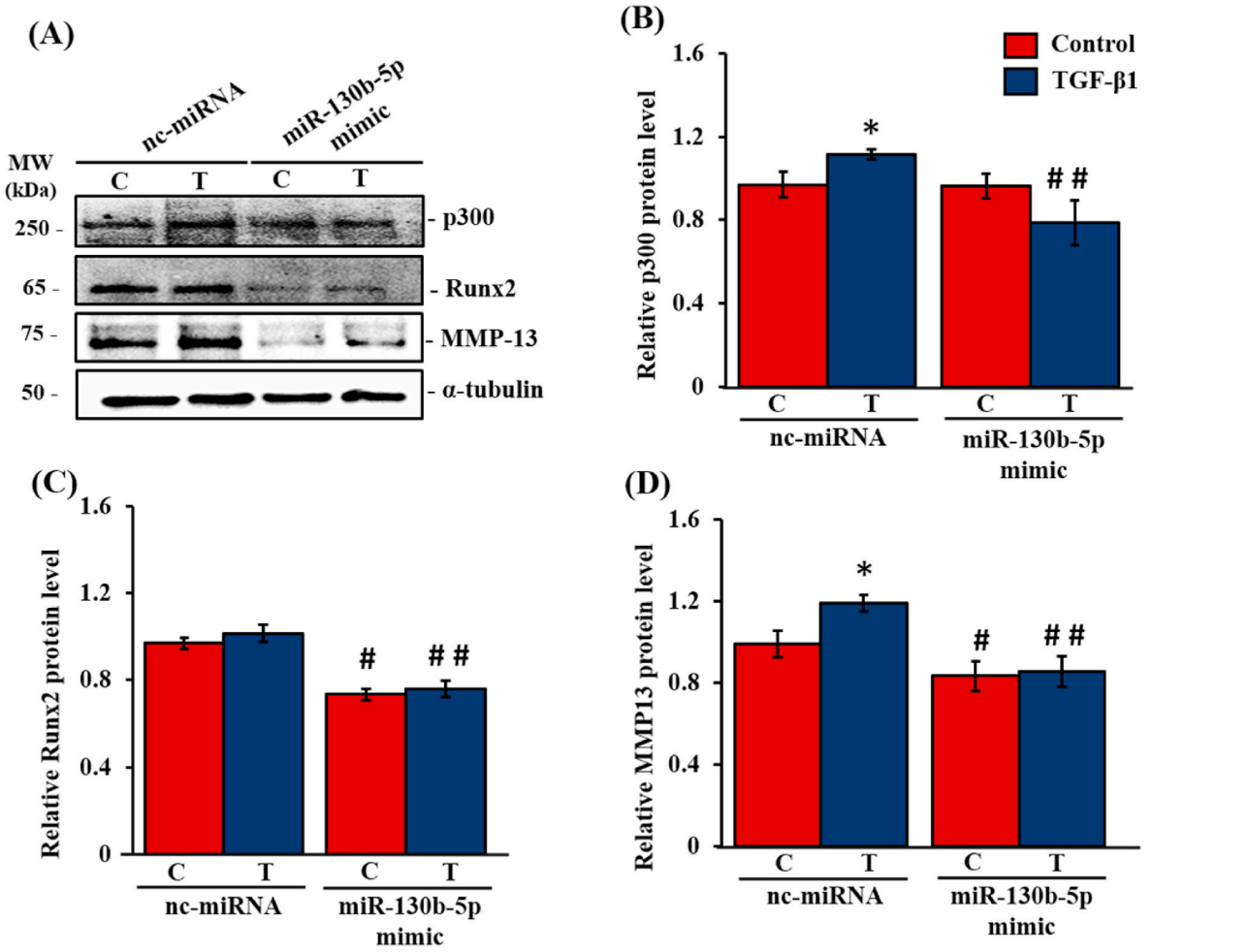

Fig. 3. Overexpression of miR-130b-5p lessened the TGF-β1-mediated stimulation of MMP-13 protein expression in rat osteoblastic cells. Transient transfection of nc-miRNA or miR-130b-5p mimic into UMR-106-01 cells for 24 h was carried out. Next, the cells were exposed to TGF-β1 for another 24 h. Using p300, Runx2, and MMP-13 antibodies, Western blot analysis was performed on the obtained whole-cell lysates. After normalization with α-tubulin, quantification of proteins was done using ImageJ software. **(A)** A representative Western blot. Expression levels of **(B)** p300 **(C)** Runx2 and **(D)** MMP-13 proteins. * Denotes a substantial increase over the corresponding control ($p < 0.01$); # Denotes a substantial reduction compared to the corresponding control under nc-miRNA transfection ($p < 0.01$); ## Indicates a statistically significant drop from the corresponding TGF-β1 treatment condition under nc-miRNA transfection ($p < 0.01$) ($n = 3$).

corresponding nc-miRNA (Fig. 2A). Even though miR-130b-5p expression was upregulated, TGF-β1 downregulated its expression, as observed in UMR-106-01 and HS-5 cells (Fig. 1B and C). These results indicated that the transient transfection of the miR-130b-5p mimic resulted in increased endogenous expression of miR-130b-5p in rat osteoblasts.

Immunoprecipitation and Western blot analyses were carried out to evaluate the functional role of miR-130b-5p in regulating p300 and its downstream target genes (*Runx2* and *MMP-13*). Rat osteoblasts were transfected transiently with the miR-130b-5p mimic or nc-miRNA for 24 h, and TGF-β1 treatment for 2 h. Whole-cell lysates were immunoprecipitated with an anti-Runx2 antibody. This was followed by an immunoblot analysis using anti-p300, anti-acetyl-lysine, and anti-Runx2 antibodies. The results indicated a significant increase in the acetylation of Runx2 (Fig. 2B and C) and p300 (Fig. 2B and E) expression after 2 h of TGF-β1 treatment. Overexpression of miR-130b-5p caused a decrease in Runx2 protein expression (Fig. 2B and D), TGF-β1-stimulated Runx2 acetylation (Fig. 2B and C), and TGF-β1-stimulated p300 (Fig. 2B and E), compared to that in the respective nc-miRNA samples in these cells. The analysis of whole-cell lysates by western blotting indicated a significant increase in p300 protein expression upon TGF-β1

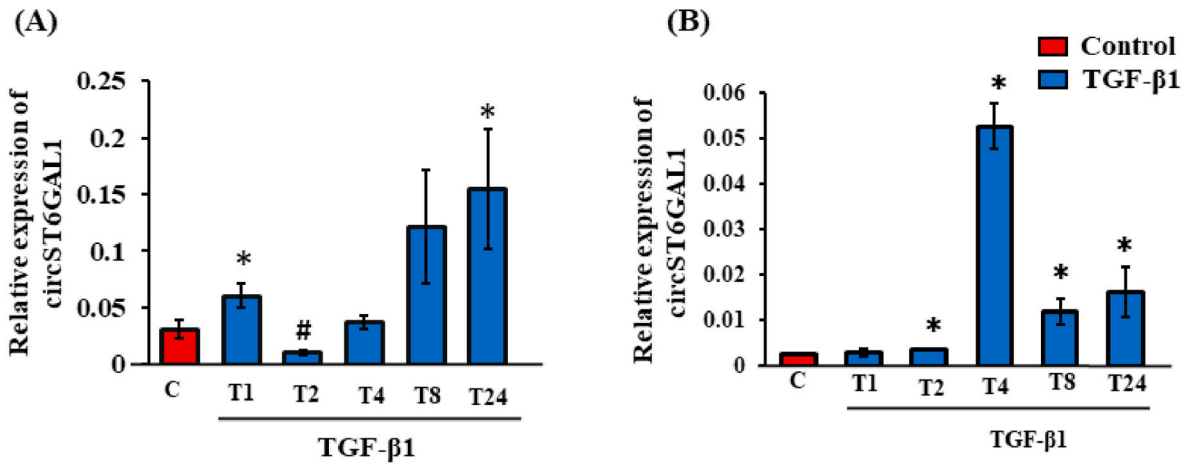

Fig. 4. TGF-β1 treatment stimulated the expression of circ_STGAL1 in osteoblastic cells. Cells were exposed with control or TGF-β1 (5 ng/ml)-containing media for 1, 2, 4, 8, or 24 h. After isolating the total RNA, qPCR testing and cDNA synthesis were performed. **(A)** Expression of circ_ST6GAL1 in UMR-106-01 cells. **(B)** Expression of circ_ST6GAL1 in rat primary osteoblasts. Internal control for normalization was RPL13AB. * Denotes a significant increase over the corresponding control ($p \leq 0.05$). # Denotes a substantial reduction compared with that in the corresponding control ($p \leq 0.05$) ($n = 3$).

treatment under nc-miRNA conditions (Fig. 2F and G), whereas, in miR-130b-5p overexpressed samples, there was a significant decrease in p300 and Runx2 protein expression (Fig. 2F, G, and H) in UMR-106-01 cells. These findings therefore showed that targeting p300 by miR-130b-5p caused a decrease in TGF-β1-stimulated p300-mediated Runx2 acetylation in rat osteoblastic cells.

Rat osteoblasts were transfected transiently with nc-miRNA or miR-130b-5p mimic for 24 h, followed by 24 h of TGF-β1 treatment, to see if the regulation of p300 by miR-130b-5p affects the TGF-β1-mediated activation of MMP-13 protein. Western blot analysis was done with whole-cell lysates, using antibodies for MMP-13, p300, and Runx2. In nc-miRNA transfected samples, TGF-β1 increased p300 (Fig. 3A and B) and MMP-13 (Fig. 3A and D) protein expression with no alteration in Runx2 expression (Fig. 3A and C) in UMR-106-01 cells. In the case of miR-130b-5p mimic-transfected samples, there was a substantial decrease in the p300 (Fig. 3A and B), MMP-13 (Fig. 3A and D) and Runx2 (Fig. 3A and C) proteins in these cells. The results reported herein (Figs. 2 and 3) suggest that miR-130b-5p can regulate p300-mediated Runx2 acetylation for MMP-13 protein expression in rat osteoblasts.

3.4. TGF-β1 stimulated the expression of circ_ST6GAL1, which possesses a binding site for miR-130b-5p, in rat osteoblasts

Since miR-130b-5p was found to be downregulated by TGF-β1, we next determined the regulatory role of other ncRNAs in influencing the function of this miRNA in osteoblasts. CircRNAs have been shown to act as ceRNAs that can sponge and block the function of miRNAs [25]. *In-silico* analysis identified 13 circRNAs that putatively targeted miR-130b-5p. To analyze the expression pattern of the identified circRNAs, RT-qPCR was performed with RNA samples obtained from control or TGF-β1 treated rat osteoblasts (UMR-106-01). We found upregulation of the three circRNAs at various time intervals of TGF-β1 treatment, compared to that in the control. Among the three circRNAs, we shortlisted circ_ST6GAL1, which showed significant upregulation at 1 and 24 h of TGF-β1 treatment in these cells (Fig. 4A). Since the UMR-106-01 cells are osteosarcoma, we confirmed the expression of circ_ST6GAL1 in rat primary osteoblasts. There was also a significant increase in circ_ST6GAL1 expression at 2, 4, 8, and 24 h of TGF-β1 treatment compared to the control (Fig. 4B).

3.5. Knockdown of circ_ST6GAL1 decreased p300, Runx2 protein expression and acetylation, and MMP-13 protein in rat osteoblasts

To validate the sponging activity of circ_ST6GAL1 and understand its subsequent effect on p300 protein and Runx2 acetylation on *MMP-13* protein expression, we performed ASO-mediated silencing of circ_ST6-GAL1. Transient transfection of UMR-106-01 cells with the circ_ST6-GAL1 ASO or negative control was performed for 24 h, followed by 2 h of control or TGF-β1 treatment. Using the Runx2 antibody, immunoprecipitation was carried out with whole-cell lysates. Next, p300, Runx2, or acetyl-lysine antibodies were used for an immunoblot analysis. The results showed that TGF-β1 stimulated the acetylation of Runx2 (Fig. 5A and B) and increased p300 protein expression (Fig. 5A and D) under negative control conditions in rat osteoblasts. Transient transfection with ASO of circ_ST6GAL1 decreased TGF-β1-stimulated Runx2 acetylation (Fig. 5A and B), Runx2 (Fig. 5A and C), and p300 protein expression (Fig. 5A and D) in these cells. Western blot analysis of aliquots of whole-cell lysates indicated that the knockdown of circ_ST6-GAL1 decreased the expression of p300 protein (Fig. 5E and F) while creating no significant change in the expression of Runx2 (Fig. 5E and G) in rat osteoblasts. These findings suggest that circ_ST6GAL1 sponges miR-130b-5p under TGF-β1 treatment and this mechanism is required for the p300-dependent Runx2 stability via acetylation for MMP-13 expression in these cells.

Next, we determined whether TGF-β1-stimulated circ_ST6GAL1 is required for the protein expression of MMP-13 in rat osteoblasts. Whole-cell lysates that had been transfected for 24 h with the negative control or ST6GAL1 ASO, followed by 8 h of control or TGF-β1 treatment, were analyzed by Western blot. Results demonstrated that under negative control and TGF-β1 treatment conditions, there was an increase in p300 (Fig. 6A and B) and MMP-13 (Fig. 6A and C) protein expression. When cells were transfected with ST6GAL1 ASO under TGF-β1 treatment conditions, p300 (Fig. 6A and B) and MMP-13 (Fig. 6A and C) expression were significantly decreased, and the expression of Runx2 (Fig. 6A and D) remained unaltered.

3.6. miR-130b-5p directly targeted the 3′ UTR of p300 and circ_ST6GAL1 in rat osteoblasts

Since overexpression of miR-130b-5p downregulated p300 expression (Figs. 2 and 3), which is essential for Runx2 acetylation, we next determined the direct targeting of the p300 3′UTR by miR-130b-5p using a dual luciferase reporter assay, as described previously [27,28]. The

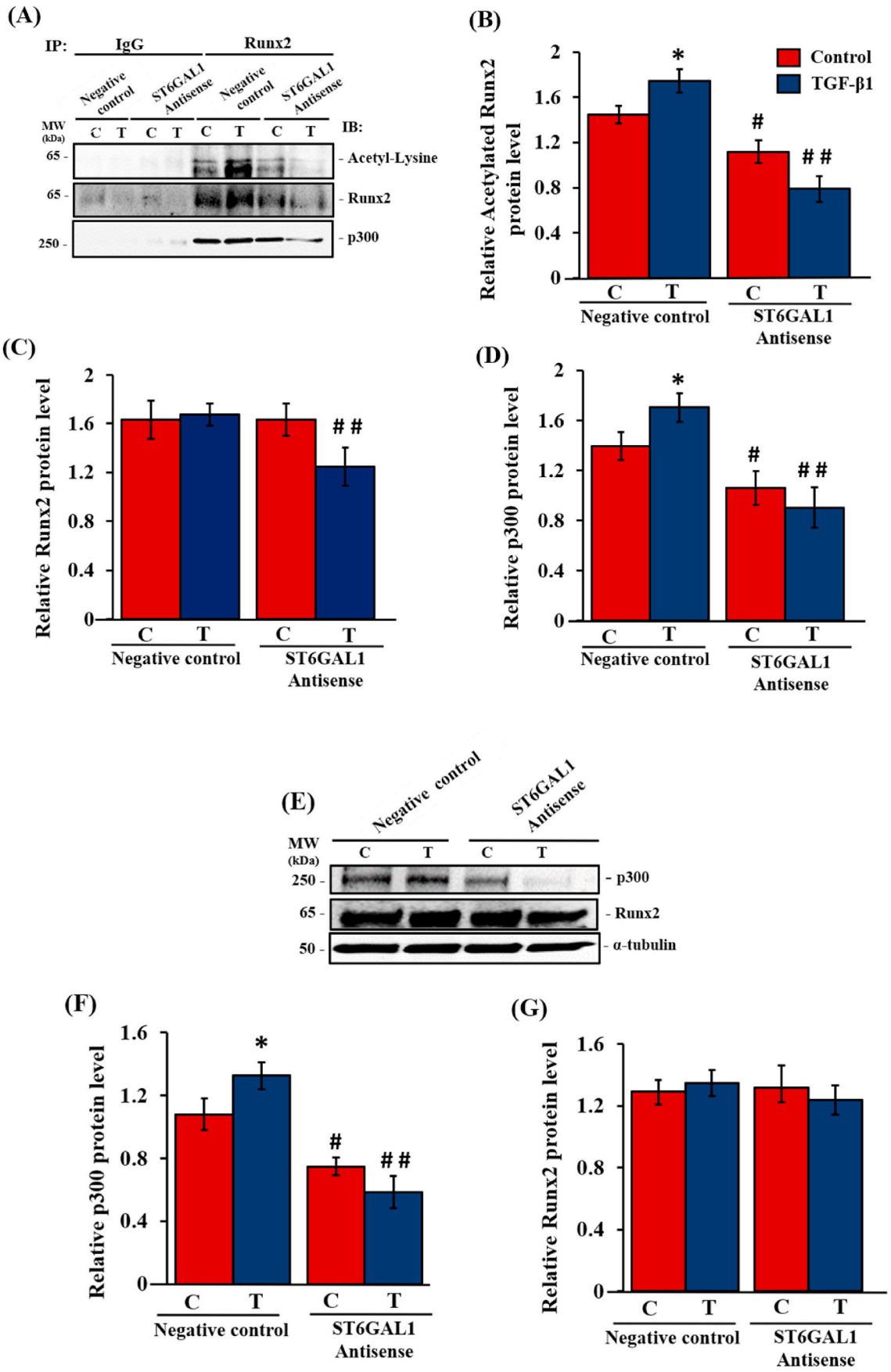

(caption on next page)

Fig. 5. Antisense-mediated inhibition of circ_ST6GAL1 decreased TGF-β1-stimulated Runx2 acetylation and p300 protein expression in rat osteoblastic cells. UMR-106-01 cells were transfected with circ_ST6GAL1 antisense (ASO) or negative control for 24 h, followed by 2 h of TGF-β1-treatment. IgG or Runx2 antibodies were used for IP after the collection of whole-cell lysates, and antibodies for Runx2, acetyl-lysine, and p300 were used for IB analysis. **(A)** A representative IP and IB blot is shown ($n = 3$). IgG was used for normalization and ImageJ software was used for quantification of proteins. **(B)** Expression levels of acetylated Runx2, **(C)** Runx2, and **(D)** p300 proteins. Using p300, Runx2, or α-tubulin antibodies, a sample of the prepared whole-cell lysates was applied to a Western blot analysis right away. After normalization with α-tubulin, quantification of proteins was done using ImageJ software. **(E)** A representative Western blot is shown. Expression levels of **(F)** p300 and **(G)** Runx2 proteins ($n = 4$). * Denotes a significant increase over the corresponding control ($p < 0.05$); # Denotes a substantial reduction compared to that in the respective negative control ($p < 0.05$); ## Denotes a substantial reduction compared to that in the respective TGF-β1-treatment under negative control transfection ($p < 0.05$).

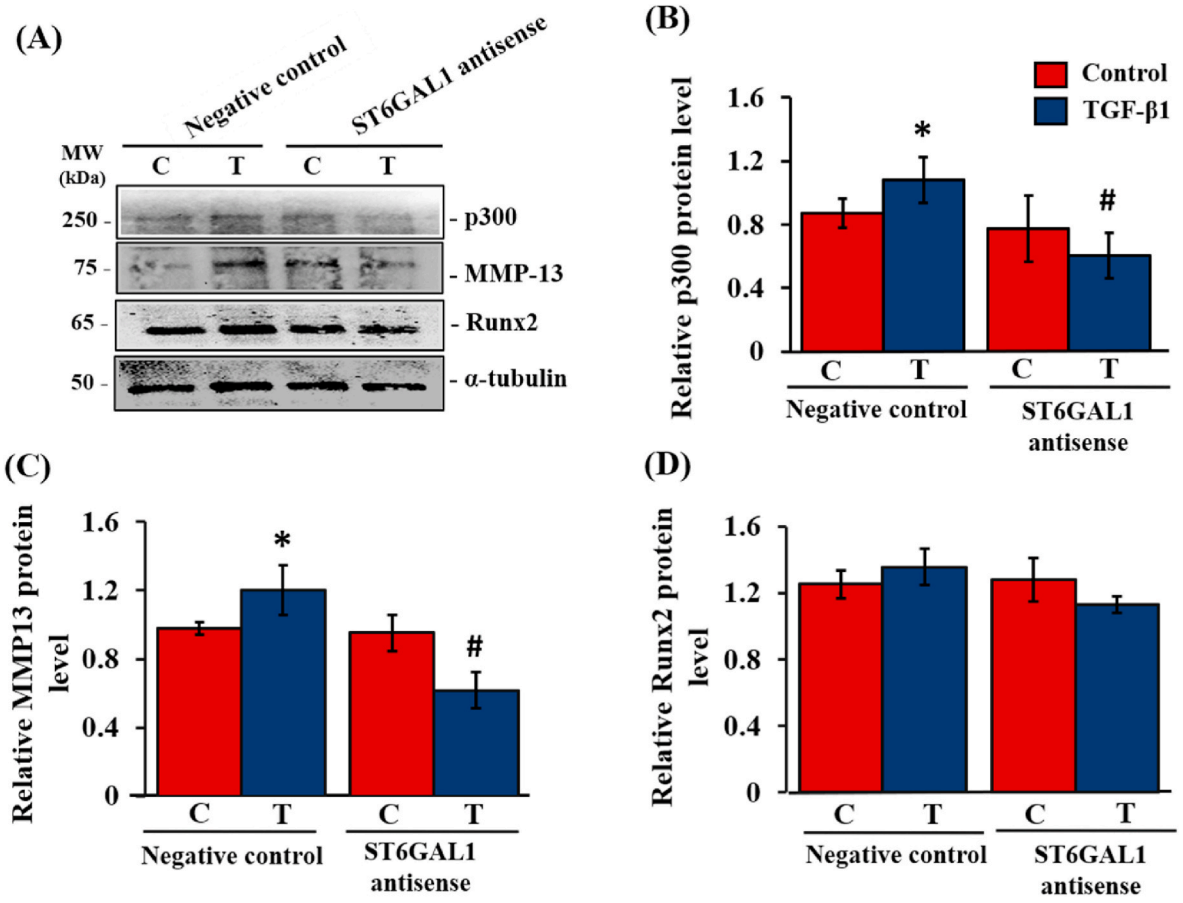

Fig. 6. Antisense-mediated inhibition of circ_ST6GAL1 decreased TGF-β1-stimulated MMP-13 expression in rat osteoblastic cells. UMR-106-01 cells were transfected transiently with negative control or ST6GAL1 antisense (ASO) for 24 h, followed by 8 h of TGF-β1 treatment. The antibodies for p300, Runx2, and MMP-13 were used in a Western blot study of whole-cell lysates. For normalization, α-tubulin was utilized, and ImageJ was used to quantify the proteins. **(A)** A representative Western blot is shown. Expression levels of **(B)** p300 **(C)** Runx2 and **(D)** MMP-13 proteins. Quantification of proteins was done using ImageJ software after normalization with α-tubulin. * Denotes a substantial increase over the corresponding control ($p < 0.05$); # Denotes a substantial reduction compared to that in the respective TGF-β1 treatment under negative control transfection ($p < 0.05$) ($n = 4$).

MREs in the WT and Mut 3′UTRs of p300 are shown in Fig. 7A. When rat osteoblasts were transiently transfected with the 3′UTR of Wt p300 in the presence of the miR-130b-5p mimic, the luciferase activity was significantly decreased. Conversely, when cells were transfected with the 3′-UTR of Mut p300 in the presence of the miR-130b-5p mimic, there was no change in luciferase activity (Fig. 7B). These results indicate the direct targeting of p300 by miR-130b-5p in rat osteoblasts.

Next, to elucidate the potential mechanism of miR-130b-5p sponging and degradation by circ_ST6GAL1, circRNA and miRNA interactions were determined using the luciferase reporter assay system. By the *in-silico* analysis, we identified three different MREs in circ_ST6GAL1 for miR-130b-5p. The MREs in the Wt and Mut circ_ST6GAL1 are shown in Fig. 7C, E, and G. Rat osteoblasts were transiently transfected with the Wt or Mut circ_ST6GAL1 constructs in the presence of the miR-130b-5p mimic or nc-miRNA. The results demonstrated a significant decrease in luciferase activity in the wild circ_ST6GAL1 (1, 2, and 3) constructs and miR-130b-5p mimic-transfected samples, whereas there were no changes in the luciferase activity in cells transfected with the Mut circ_ST6GAL1 (1, 2, and 3) constructs and miR-130b-5p mimic or nc-miRNA (Fig. 7D, F, and H). These results confirmed the direct binding of all three MREs in circ_ST6GAL1 to miR-130b-5p in rat osteoblasts.

4. Discussion

Osteoblasts and osteoclasts both produce MMPs, a class of zinc-dependent proteolytic enzymes that play a role in ECM remodeling. In particular, MMP2, MMP9, MMP-13, and MMP14 are crucial for bone development and remodeling [15,29]. Considering their essentiality in the initial modeling and development of long bones [30–32], the expression of MMP-13 is observed to be enhanced in osteoblasts. MMP-13 is also capable of binding to the collagen matrix and controlling collagen remodeling [33]. Mice lacking MMP-13 develop aberrant bone

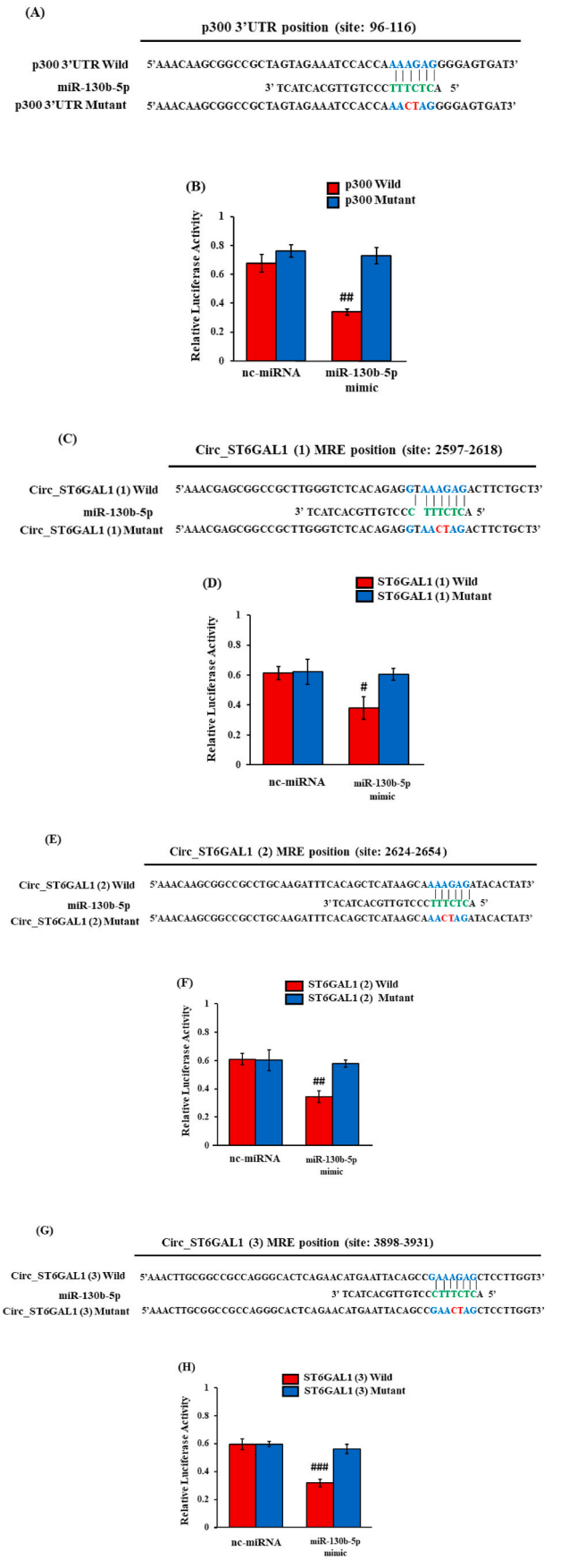

(caption on next column)

Fig. 7. Direct binding of miR-130b-5p with the 3′ UTR of p300 and circ_ST6GAL1 in rat osteoblastic cells. A pictorial representation of binding between the miR-130b-5p with the **(A)** 3′ UTR of p300 **(C)** Circ-ST6GAL1 (1) **(E)** Circ-ST6GAL1 (2) **(G)** Circ-ST6GAL1 (3) (wild and mutated binding sites). Nucleotides represented in blue and red are MRE and mutated MRE, respectively. Nucleotides represented in green are miR-130b-5p seed site. UMR-106-01 cells were transfected with 1 μg pmirGLO construct containing wild or mutant **(B)** 3′ UTR of p300, **(D)** Circ_ST6GAL1 (1), **(F)** Circ_ST6GAL1 (2) or **(H)** Circ_ST6GAL1 (3) in the presence of 50 nM of nc-miRNA or miR-130b-5p mimic. After 24 h, lysates were prepared. After normalizing with Renilla luciferase activity, Firefly luciferase activity was measured. # Denotes a substantial decrease compared to that in the corresponding nc-miRNA-transfected cells ($p < 0.05$). ## Denotes a substantial reduction comparing the respective nc-miRNA transfected cells ($p < 0.005$). ### Denotes a substantial reduction comparing the respective nc-miRNA transfected cells ($p < 0.001$) ($n = 3$).

morphologies, such as endochondral bone malformation [34,35], thereby exhibiting less potential to heal long-bone fractures [36]. Furthermore, Runx2, an osteogenic marker, targets the promoter of *MMP-13* thereby regulating its gene expression [32,37]. Any mutations in the *Runx2* gene can cause CCD, a crucial transcription factor required for bone development [12,38]. Runx2 activity can be regulated by a number of signaling pathways (TGF-β, BMP, PTH, and Wnt) [5,39–41] and several phytocompounds (diosmin and sinapic acid) [42,43]. Our earlier findings showed that Runx2 undergoes post-translational modifications (phosphorylation and acetylation), in response to TGF-β1 stimulation in osteoblasts [10,15]. Runx2 phosphorylation may be subject to proteasomal degradation; however, its acetylation protects Runx2 from degradation [44,45]. In histones, transcription factors and non-histone proteins, HATs and histone deacetylases (HDACs), influence acetylation and deacetylation, respectively. Both have been reported to interact with Runx2 and modulate its stability in cells [16,46,47].

In response to TGF-β1, p300, a HAT and transcriptional coactivator, was found to promote Runx2 acetylation and consequently facilitate *MMP-13* transcription in bone-forming osteoblasts [16,17]. The bone-remodeling process can be understood in detail using the post-transcriptional regulation of p300. Earlier work demonstrated that miR-132-3p directly targets p300 and decreases its protein expression, which then decreases Runx2 acetylation, thereby impeding osteoblast development [48]. Several miRNAs, including miR-15b [49] and miR-135-5p [50] have been shown to influence osteoblast differentiation and activity via multiple pathways. In osteoblastic cells, miR-181a [51] and miR-27a [52] influence osteoblast development under TGF-β1 treatment. To our best of knowledge, no reports are available on the role of miR-130b-5p in the regulation of TGF-β1-stimulated p300 expression, Runx2 acetylation, and MMP-13 expression in osteoblasts.

In-silico analysis identified four unvalidated miRNAs that putatively target p300. Their expression was upregulated or downregulated upon TGF-β1 treatment in osteoblasts. Among these miRNAs, the expression of mir-130b and miR-130b-5p was most effectively downregulated by TGF-β1 treatment in these cells (Fig. 1). Evidence indicates that the expression of precursor and mature miRNAs may differ [53–55]. However, this was not the case in this study. miR-130b-5p expression was consistent at both precursor and mature expression in osteoblasts. The functional role of miR-130b-5p was determined by targeting p300 via overexpression of miR-130b-5p and its subsequent effects on the expression of Runx2 and its acetylation and MMP-13 expression in osteoblasts. A luciferase reporter assay identified direct targeting of the 3′UTR p300 by miR-130b-5p in rat osteoblasts (Fig. 7B). This assay system has already been used to determine direct interactions between miRNAs and their target genes [56,57]. Targeting p300 by the miR-130b-5p mimic caused a decrease in Runx2 acetylation (Fig. 2B and C), suggesting that the interaction of p300 with Runx2 is essential for Runx2 acetylation and its stability. Runx2's phosphorylation was previously demonstrated to be increased by TGF-β1 [11], and phosphorylated proteins may be vulnerable to proteasomal degradation [44,58].

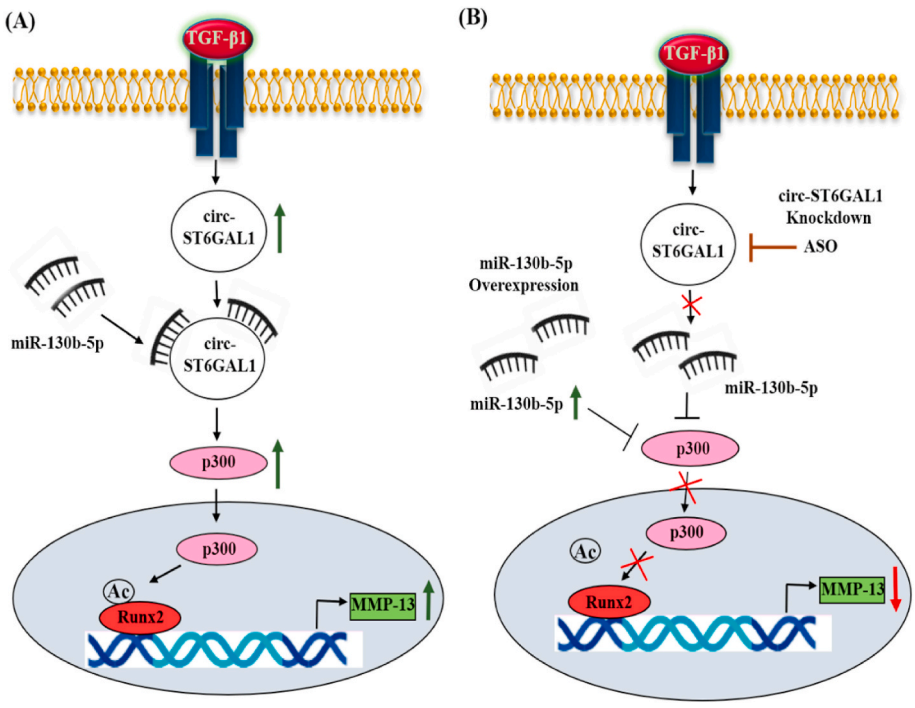

Fig. 8. Schematic representation of TGF-β1-stimulated MMP-13 expression via Runx2 acetylation through the circ-ST6GAL1/miR-130b-5p/p300 axis. (A) TGF-β1-mediated upregulation of circ-ST6GAL1 and downregulation of miR-130b-5p, increased p300 expression, which led to increased Runx2 acetylation, followed by increased MMP-13 expression in rat osteoblastic cells. **(B)** Overexpression of miR-130b-5p or ASO-mediated knockdown of circ-ST6GAL1 decreased p300 expression, which led to decreased Runx2 acetylation, followed by decreased MMP-13 expression in rat osteoblastic cells. ↑ indicates Upregulation; ↓ indicates downregulation.

Acetylation could prevent the degradation of the phosphorylated proteins by masking their lysine residues with acetyl groups, thus preventing the attachment of the ubiquitin residues and proteasomal degradation [59]. Runx2 undergoes several modifications, such as acetylation, ubiquitination, and glycosylation, in response to various treatments such as TGF-β1, PTH, BMP, and TNF [16,60–62]. In the present investigation, we found that Runx2 acetylation by TGF-β1 treatment was mediated by the downregulation of p300 targeting miR-130b-5p (Fig. 2), and this effect was found to be essential for MMP-13 expression in osteoblasts (Fig. 3).

There is interplay among various ncRNAs that control their target gene expression. circRNAs act as ceRNAs, thus, regulating the activity of miRNAs [63]. For instance, circ_0000020 supports osteogenic differentiation to prevent osteoporosis by sponging miR-142-5p and upregulating BMP2 [64]. Similar to this, the hsa_circ_0006766–miR-4739–Notch2 axis controls the MAPK signaling pathway to support osteogenic differentiation [65]. Using bioinformatics tools, we found that circ_ST6GAL1 has MREs for miR-130b-5p. The expression of circ_ST6GAL1 was also upregulated upon TGF-β1 treatment in rat osteoblasts (Fig. 4). Furthermore, the knockdown of circ_ST6GAL1 resulted in the unblocking of miR-130b-5p, which caused the downregulation of p300, resulting in decreased Runx2 acetylation and MMP-13 expression upon TGF-β1 treatment in rat osteoblasts (Figs. 5 and 6). CircRNAs may contain more than one MRE [66], and we predicted three different binding sites for miR-130b-5p in circ_ST6GAL1. The presence of more than one MRE in circRNAs may increase their sponging activity towards miRNAs, and hence, a smaller number of circRNAs may be required to regulate the miRNA expression [67,68]. The luciferase reporter assay revealed that miR-130b-5p directly interacted with circ_ST6GAL1 at all three predicted MREs (Fig. 7). The direct interaction of circRNAs with miRNAs has previously been identified using luciferase reporter assays [69–71]. CircRNAs serve as miRNA sponges to inhibit miRNA activity and regulate the expression of target genes [72–75]. miRNAs have the potential to target more than one gene; similarly, one miRNA can be targeted or sponged by more than one circRNA [76–78]. For example, miR-130b-5p was also sponged by circ_CUX1 under PTH treatment in osteoblasts [79]. This type of regulation is essential for regulating various cellular activities under physiological conditions [80,81], and dysfunction in the interaction of these ncRNAs may lead to pathological conditions [82–84].

Taken together, our data indicate that TGF-β1-treatment stimulates the expression of p300 via the stimulation of circ_ST6GAL1 expression and its sponging activity towards miR-130b-5p in osteoblasts. The overexpression of miR-130b-5p and knockdown of circ_ST6GAL1 reversed the effect of TGF-β1 on MMP-13 expression via p300-mediated Runx2 acetylation in rat osteoblasts (Fig. 8). Our results show that the circ_ST6GAL1/miR-130b-5p/p300 axis plays a pivotal role in regulating Runx2 acetylation and MMP-13 expression and has potential therapeutic application in bone and bone-related diseases.

Data availability

The corresponding author will provide the results produced during the current investigation upon reasonable request.

CRediT authorship contribution statement

I. Saranya: Investigation, Methodology, Validation, Writing – original draft. **R.L. Akshaya:** Data curation, Formal analysis, Methodology. **K. Gomathi:** Conceptualization, Investigation, Validation. **R. Mohanapriya:** Conceptualization, Formal analysis. **Z. He:** Data curation, Methodology. **N.C. Partridge:** Formal analysis, Resources. **N. Selvamurugan:** Conceptualization, Funding acquisition, Investigation, Project administration, Resources, Supervision, Validation, Writing – review & editing.

Declaration of competing interest

The authors declare that they have no known competing financial interests or personal relationships that could have appeared to influence the work reported in this paper.

Acnowledgements

The Indian Council of Medical Research (2020-0282/SCR/ADHOC-BMS to N.S.) and the Department of Science and Technology (DST/INSPIRE Fellowships: 2021/IF210073 to I. S. and 2019/IF190170 to R. L. A.) provided funding for this research.

Appendix A. Suppislementary data

Supplementary data to this article can be found online at https://doi.org/10.1016/j.ncrna.2023.11.002.

References

[1] Florencio Silva, R. Sasso, G.R. Sasso Cerri, et al., Biology of bone tissue: structure, function, and factors that influence bone cells, BioMed Res. Int. 2015 (2015), 421746, https://doi.org/10.1155/2015/421746.
[2] J. Scheinpflug, M. Pfeiffenberger, A. Damerau, et al., Journey into bone models: a review, Genes 9 (5) (2018) 247, https://doi.org/10.3390/genes9050247.
[3] P. Katsimbri, The biology of normal bone remodeling, Eur. J. Cancer Care 26 (6) (2017), https://doi.org/10.1111/ecc.12740, 10.1111/ecc.12740.
[4] D.J. Hadjidakis, I.I. Androulakis, Bone remodeling, Ann. N. Y. Acad. Sci. 1092 (2006) 385–396, https://doi.org/10.1196/annals.1365.035.
[5] I. Saranya, R.L. Akshaya, N. Selvamurugan, Regulation of Wnt signaling by non-coding RNAs during osteoblast differentiation, Different.; Res. Biol. Diversity 128 (2022) 57–66, https://doi.org/10.1016/j.diff.2022.10.003.
[6] A. Poniatowski Ł, P. Wojdasiewicz, R. Gasik, et al., Transforming growth factor Beta family: insight into the role of growth factors in regulation of fracture healing biology and potential clinical applications, Mediat. Inflamm. 2015 (2015), 137823, https://doi.org/10.1155/2015/137823.
[7] J.L. Crane, X. Cao, Bone marrow mesenchymal stem cells and TGF-β signaling in bone remodeling, J. Clin. Invest. 124 (2) (2014) 466–472, https://doi.org/10.1172/JCI70050.
[8] A. Aiken, R. Khokha, Unraveling metalloproteinase function in skeletal biology and disease using genetically altered mice, Biochim. Biophys. Acta 1803 (1) (2010) 121–132, https://doi.org/10.1016/j.bbamcr.2009.07.002.
[9] N. Selvamurugan, S. Kwok, T. Alliston, et al., Transforming growth factor-beta 1 regulation of collagenase-3 expression in osteoblastic cells by cross-talk between the Smad and MAPK signaling pathways and their components, Smad2 and Runx2, J. Biol. Chem. 279 (18) (2004) 19327–19334, https://doi.org/10.1074/jbc.M314048200.
[10] N. Selvamurugan, E. Shimizu, M. Lee, et al., Identification and characterization of Runx2 phosphorylation sites involved in matrix metalloproteinase-13 promoter activation, FEBS Lett. 583 (7) (2009) 1141–1146, https://doi.org/10.1016/j.febslet.2009.02.040.
[11] B. Arumugam, M. Vairamani, N.C. Partridge, et al., Characterization of Runx2 phosphorylation sites required for TGF-β1-mediated stimulation of matrix metalloproteinase-13 expression in osteoblastic cells, J. Cell. Physiol. 233 (2) (2018) 1082–1094, https://doi.org/10.1002/jcp.25964.
[12] S. Yoda, N. Suda, Y. Kitahara, et al., Delayed tooth eruption and suppressed osteoclast number in the eruption pathway of heterozygous Runx2/Cbfa1 knockout mice, Arch. Oral Biol. 49 (6) (2004) 435–442, https://doi.org/10.1016/j.archoralbio.2004.01.010.
[13] T.M. Schroeder, E.D. Jensen, J.J. Westendorf, Runx2: a master organizer of gene transcription in developing and maturing osteoblasts, Birth Defects Res. Part C Embryo Today - Rev. 75 (3) (2005) 213–225, https://doi.org/10.1002/bdrc.20043.
[14] M.J. Jiménez, M. Balbín, J.M. López, et al., Collagenase 3 is a target of Cbfa1, a transcription factor of the runt gene family involved in bone formation, Mol. Cell Biol. 19 (6) (1999) 4431–4442, https://doi.org/10.1128/MCB.19.6.4431.
[15] D.J. Behonick, Z. Xing, S. Lieu, et al., Role of matrix metalloproteinase 13 in both endochondral and intramembranous ossification during skeletal regeneration, PLoS One 2 (11) (2007) e1150.
[16] K. Gomathi, M. Rohini, N.C. Partridge, et al., Regulation of transforming growth factor-β1-stimulation of Runx2 acetylation for matrix metalloproteinase 13 expression in osteoblastic cells, Biol. Chem. 403 (3) (2021) 305–315, https://doi.org/10.1515/hsz-2021-0292.
[17] K. Gomathi, M. Rohini, M. Vairamani, et al., Identification and characterization of TGF-β1-responsive Runx2 acetylation sites for matrix Metalloproteinase-13 expression in osteoblastic cells, Biochimie 201 (2022) 1–6, https://doi.org/10.1016/j.biochi.2022.06.013.
[18] K. Gomathi, N. Akshaya, N. Srinaath, et al., Histone acetyl transferases and their epigenetic impact on bone remodeling, Int. J. Biol. Macromol. 170 (2021) 326–335, https://doi.org/10.1016/j.ijbiomac.2020.12.173.
[19] S. Vimalraj, N. Selvamurugan, MicroRNAs: synthesis, gene regulation and osteoblast differentiation, Curr. Issues Mol. Biol. 15 (2013) 7–18.
[20] Y. Yang, S. Fang, Small non-coding RNAs-based bone regulation and targeting therapeutic strategies, Mol. Cell. Endocrinol. 456 (2017) 16–35, https://doi.org/10.1016/j.mce.2016.11.018.
[21] S. Jonas, E. Izaurralde, Towards a molecular understanding of microRNA-mediated gene silencing, Nat. Rev. Genet. 16 (7) (2015) 421–433, https://doi.org/10.1038/nrg3965.
[22] X. Zhao, D. Xu, Y. Li, et al., MicroRNAs regulate bone metabolism, J. Bone Miner. Metabol. 32 (3) (2014) 221–231, https://doi.org/10.1007/s00774-013-0537-7.
[23] R.L. Akshaya, N. Akshaya, N. Selvamurugan, A computational study of non-coding RNAs on the regulation of activating transcription factor 3 in human breast cancer cells, Comput. Biol. Chem. 89 (2020), 107386, https://doi.org/10.1016/j.compbiolchem.2020.107386.
[24] R.A. Wesselhoeft, P.S. Kowalski, D.G. Anderson, Engineering circular RNA for potent and stable translation in eukaryotic cells, Nat. Commun. 9 (1) (2018) 2629, https://doi.org/10.1038/s41467-018-05096-6.
[25] M. Li, C. Li, H. Zheng, et al., CircRNA_0001795 sponges miRNA-339-5p to regulate yes-associated protein 1 expression and attenuate osteoporosis progression, Bioengineered 13 (2) (2022) 2803–2815, https://doi.org/10.1080/21655979.2021.2022074.
[26] V. Mohanakrishnan, A. Balasubramanian, G. Mahalingam, et al., Parathyroid hormone-induced down-regulation of miR-532-5p for matrix metalloproteinase-13 expression in rat osteoblasts, J. Cell. Biochem. 119 (7) (2018) 6181–6193, https://doi.org/10.1002/jcb.26827.
[27] D. Malavika, S. Shreya, V. Raj Priya, et al., miR-873-3p targets HDAC4 to stimulate matrix metalloproteinase-13 expression upon parathyroid hormone exposure in rat osteoblasts, J. Cell. Physiol. 235 (11) (2020) 7996–8009, https://doi.org/10.1002/jcp.29454.
[28] N. Akshaya, N. Srinaath, M. Rohini, et al., Parathyroid hormone-regulation of Runx2 by MiR-290 for matrix metalloproteinase-13 expression in rat osteoblastic cells, Curr. Mol. Med. 22 (6) (2022) 549–561, https://doi.org/10.2174/1566524021666210830093232.
[29] K.B. Paiva, J.M. Granjeiro, Bone tissue remodeling and development: focus on matrix metalloproteinase functions, Arch. Biochem. Biophys. 561 (2014) 74–87, https://doi.org/10.1016/j.abb.2014.07.034.
[30] V. Mattot, M.B. Raes, P. Henriet, et al., Expression of interstitial collagenase is restricted to skeletal tissue during mouse embryogenesis, J. Cell Sci. 108 (Pt 2) (1995) 529–535, https://doi.org/10.1242/jcs.108.2.529.
[31] X. Wang, P.A. Manner, A. Horner, et al., Regulation of MMP-13 expression by RUNX2 and FGF2 in osteoarthritic cartilage, Osteoarthritis Cartilage 12 (12) (2004) 963–973, https://doi.org/10.1016/j.joca.2004.08.008.
[32] Q. Wu, K. Wang, X. Wang, et al., Delivering siRNA to control osteogenic differentiation and real-time detection of cell differentiation in human mesenchymal stem cells using multifunctional gold nanoparticles, J. Mater. Chem. B 8 (15) (2020) 3016–3027, https://doi.org/10.1039/c9tb02899d.
[33] J.M. Howes, D. Bihan, D.A. Slatter, et al., The recognition of collagen and triple-helical toolkit peptides by MMP-13: sequence specificity for binding and cleavage, J. Biol. Chem. 289 (35) (2014) 24091–24101, https://doi.org/10.1074/jbc.M114.583443.
[34] S. Barthelemi, J. Robinet, R. Garnotel, et al., Mechanical forces-induced human osteoblasts differentiation involves MMP-2/MMP-13/MT1-MMP proteolytic cascade, J. Cell. Biochem. 113 (3) (2012) 760–772, https://doi.org/10.1002/jcb.23401.
[35] S.Y. Tang, R.P. Herber, S.P. Ho, et al., Matrix metalloproteinase-13 is required for osteocytic perilacunar remodeling and maintains bone fracture resistance, J. Bone Miner. Res. : Off. J. Am. Soc. Bone Mineral Res. 27 (9) (2012) 1936–1950, https://doi.org/10.1002/jbmr.1646.
[36] N. Kosaki, H. Takaishi, S. Kamekura, et al., Impaired bone fracture healing in matrix metalloproteinase-13 deficient mice, Biochem. Biophys. Res. Commun. 354 (4) (2007) 846–851, https://doi.org/10.1016/j.bbrc.2006.12.234.
[37] J. Yue, K. Zhang, J. Chen, Role of integrins in regulating proteases to mediate extracellular matrix remodeling, Cancer Microenviron 5 (3) (2012) 275–283.
[38] K.E. Lee, F. Seymen, J. Ko, et al., RUNX2 mutations in cleidocranial dysplasia, Genet. Mol. Res.: GMR 12 (4) (2013) 4567–4574, https://doi.org/10.4238/2013.October.15.5.
[39] K.S. Lee, H.J. Kim, Q.L. Li, et al., Runx2 is a common target of transforming growth factor beta1 and bone morphogenetic protein 2, and cooperation between Runx2 and Smad5 induces osteoblast-specific gene expression in the pluripotent mesenchymal precursor cell line C2C12, Mol. Cell Biol. 20 (23) (2000) 8783–8792, https://doi.org/10.1128/MCB.20.23.8783-8792.2000.
[40] M. Wu, G. Chen, Y.P. Li, TGF-β and BMP signaling in osteoblast, skeletal development, and bone formation, homeostasis and disease, Bone Res. 4 (2016), 16009, https://doi.org/10.1038/boneres.2016.9.
[41] B. Arumugam, M. Vishal, S. Shreya, et al., Parathyroid hormone-stimulation of Runx2 during osteoblast differentiation via the regulation of lnc-SUPT3H-1:16 (RUNX2-AS1:32) and miR-6797-5p, Biochimie 158 (2019) 43–52, https://doi.org/10.1016/j.biochi.2018.12.006.
[42] S.V. Chandran, M. Vairamani, N. Selvamurugan, Osteostimulatory effect of biocomposite scaffold containing phytomolecule diosmin by Integrin/FAK/ERK signaling pathway in mouse mesenchymal stem cells, Sci. Rep. 9 (1) (2019), 11900, https://doi.org/10.1038/s41598-019-48429-1.
[43] K. Balagangadharan, R. Trivedi, M. Vairamani, et al., Sinapic acid-loaded chitosan nanoparticles in polycaprolactone electrospun fibers for bone regeneration in vitro and in vivo, Carbohydr. Polym. 216 (2019) 1–16, https://doi.org/10.1016/j.carbpol.2019.04.002.

[44] T. Ravid, M. Hochstrasser, Diversity of degradation signals in the ubiquitin-proteasome system, Nat. Rev. Mol. Cell Biol. 9 (9) (2008) 679–690, https://doi.org/10.1038/nrm2468.
[45] A. Drazic, L.M. Myklebust, R. Ree, et al., The world of protein acetylation, Biochim. Biophys. Acta 1864 (10) (2016) 1372–1401, https://doi.org/10.1016/j.bbapap.2016.06.007.
[46] M. Bruderer, R.G. Richards, M. Alini, et al., Role and regulation of RUNX2 in osteogenesis, Eur. Cell. Mater. 28 (2014) 269–286, https://doi.org/10.22203/ecm.v028a19.
[47] K.L. Norris, J.Y. Lee, T.P. Yao, Acetylation goes global: the emergence of acetylation biology, Sci. Signal. 2 (97) (2009) pe76, https://doi.org/10.1126/scisignal.297pe76.
[48] Z. Hu, Y. Wang, Z. Sun, et al., miRNA-132-3p inhibits osteoblast differentiation by targeting Ep300 in simulated microgravity, Sci. Rep. 5 (2015), 18655, https://doi.org/10.1038/srep18655.
[49] S. Vimalraj, N.C. Partridge, N. Selvamurugan, A positive role of microRNA-15b on regulation of osteoblast differentiation, J. Cell. Physiol. 229 (9) (2014) 1236–1244, https://doi.org/10.1002/jcp.24557.
[50] N. Yin, L. Zhu, L. Ding, et al., MiR-135-5p promotes osteoblast differentiation by targeting HIF1AN in MC3T3-E1 cells, Cell. Mol. Biol. Lett. 24 (2019) 51, https://doi.org/10.1186/s11658-019-0177-6.
[51] R. Bhushan, J. Grünhagen, J. Becker, et al., miR-181a promotes osteoblastic differentiation through repression of TGF-β signaling molecules, Int. J. Biochem. Cell Biol. 45 (3) (2013) 696–705, https://doi.org/10.1016/j.biocel.2012.12.008.
[52] Y. Bai, Y. Liu, S. Jin, et al., Expression of microRNA-27a in a rat model of osteonecrosis of the femoral head and its association with TGF-β/Smad7 signaling in osteoblasts, Int. J. Mol. Med. 43 (2) (2019) 850–860, https://doi.org/10.3892/ijmm.2018.4007.
[53] E.J. Lee, M. Baek, Y. Guse, et al., Systematic evaluation of microRNA processing patterns in tissues, cell lines, and tumors, RNA 14 (1) (2008) 35–42, https://doi.org/10.1261/rna.804508.
[54] L. Gan, B. Denecke, Profiling pre-MicroRNA and mature MicroRNA expressions using a single microarray and avoiding separate sample preparation, Microarrays 2 (1) (2013) 24–33, https://doi.org/10.3390/microarrays2010024.
[55] T.D. Schmittgen, E.J. Lee, J. Jiang, et al., Real-time PCR quantification of precursor and mature microRNA, Methods 44 (1) (2008) 31–38, https://doi.org/10.1016/j.ymeth.2007.09.006.
[56] R.L. Akshaya, M. Rohini, Z. He, et al., MiR-4638-3p regulates transforming growth factor-β1-induced activating transcription factor-3 and cell proliferation, invasion, and apoptosis in human breast cancer cells, Int. J. Biol. Macromol. 222 (Pt B) (2022) 1974–1982, https://doi.org/10.1016/j.ijbiomac.2022.09.286.
[57] M. Rohini, M. Gokulnath, P.J. Miranda, et al., miR-590-3p inhibits proliferation and promotes apoptosis by targeting activating transcription factor 3 in human breast cancer cells, Biochimie 154 (2018) 10–18, https://doi.org/10.1016/j.biochi.2018.07.023.
[58] A.C. Ventura, S.D. Merajver, X.N. Lin, Multisite phosphorylation provides an effective and flexible mechanism for switch-like protein degradation, PLoS One 5 (12) (2010), e14029.
[59] A. Drazic, L.M. Myklebust, R. Ree, et al., The world of protein acetylation, Biochim. Biophys. Acta 1864 (10) (2016) 1372–1401, https://doi.org/10.1016/j.bbapap.2016.06.007.
[60] C.E. Boumah, M. Lee, N. Selvamurugan, et al., Runx2 recruits p300 to mediate parathyroid hormone's effects on histone acetylation and transcriptional activation of the matrix metalloproteinase-13 gene, Mol. Endocrinol. (Baltimore, Md 23 (8) (2009) 1255–1263, https://doi.org/10.1210/me.2008-0217.
[61] K. Gomathi, N. Akshaya, N. Srinaath, et al., Regulation of Runx2 by post-translational modifications in osteoblast differentiation, Life Sci. 245 (2020), 117389, https://doi.org/10.1016/j.lfs.2020.117389. Kim.
[62] Hj, W.J. Kim, H.M. Ryoo, Post-translational regulations of transcriptional activity of RUNX2, Mol. Cell. 43 (2) (2020) 160–167, https://doi.org/10.14348/molcells.2019.0247.
[63] W. Shen, B. Sun, C. Zhou, et al., CircFOXP1/FOXP1 promotes osteogenic differentiation in adipose-derived mesenchymal stem cells and bone regeneration in osteoporosis via miR-33a-5p, J. Cell Mol. Med. 24 (21) (2020) 12513–12524, https://doi.org/10.1111/jcmm.15792.
[64] R. Zhou, S. Miao, J. Xu, et al., Circular RNA circ_0000020 promotes osteogenic differentiation to reduce osteoporosis via sponging microRNA miR-142-5p to up-regulate Bone Morphogenetic Protein BMP2, Bioengineered 12 (1) (2021) 3824–3836, https://doi.org/10.1080/21655979.2021.1949514.
[65] Z. Guo, M. Xie, Y. Zou, et al., Circular RNA Hsa_circ_0006766 targets microRNA miR-4739 to regulate osteogenic differentiation of human bone marrow mesenchymal stem cells, Bioengineered 12 (1) (2021) 5679–5687, https://doi.org/10.1080/21655979.2021.1967712.
[66] C.Y. Yu, H.C. Kuo, The emerging roles and functions of circular RNAs and their generation, J. Biomed. Sci. 26 (1) (2019) 29, https://doi.org/10.1186/s12929-019-0523-z.
[67] S. Dodbele, N. Mutlu, J.E. Wilusz, Best practices to ensure robust investigation of circular RNAs: pitfalls and tips, EMBO Rep. 22 (3) (2021), e52072, https://doi.org/10.15252/embr.202052072.
[68] X. Chen, T. Yang, W. Wang, et al., Circular RNAs in immune responses and immune diseases, Theranostics 9 (2) (2019) 588–607, https://doi.org/10.7150/thno.29678.PMID:30809295. PMCID: PMC6376182.
[69] Y. Li, B. Chen, S. Huang, Identification of circRNAs for miRNA targets by Argonaute2 RNA immunoprecipitation and luciferase screening assays, Methods Mol. Biol. 1724 (2018) 209–218, https://doi.org/10.1007/978-1-4939-7562-4_17.
[70] J.D.C. Tian, L. Liang, Involvement of circular RNA SMARCA5/microRNA-620 axis in the regulation of cervical cancer cell proliferation, invasion and migration, Eur. Rev. Med. Pharmacol. Sci. 22 (24) (2018) 8589–8598, https://doi.org/10.26355/eurrev_201812_16622.
[71] L. Zhu, Y. Liu, Y. Yang, et al., CircRNA ZNF609 promotes growth and metastasis of nasopharyngeal carcinoma by competing with microRNA-150-5p, Eur. Rev. Med. Pharmacol. Sci. 23 (7) (2019) 2817–2826, https://doi.org/10.26355/eurrev_201904_17558.
[72] R. Saikishore, P. Velmurugan, D. Ranjithkumar, et al., The circular RNA-miRNA Axis: a special RNA signature regulatory transcriptome as a potential biomarker for OSCC, Mol. Ther. Nucleic Acids 22 (2020) 352–361, https://doi.org/10.1016/j.omtn.2020.09.001.
[73] R. Mohanapriya, R.L. Akshaya, N. Selvamurugan, A regulatory role of circRNA-miRNA-mRNA network in osteoblast differentiation, Biochimie 193 (2022) 137–147, https://doi.org/10.1016/j.biochi.2021.11.001.
[74] A. Lavenniah, T.D.A. Luu, Y.P. Li, et al., Engineered circular RNA sponges act as miRNA inhibitors to attenuate pressure overload-induced cardiac hypertrophy, Mol. Ther. : J. Am. Soc. Gene Therapy 28 (6) (2020) 1506–1517, https://doi.org/10.1016/j.ymthe.2020.04.006.
[75] S. Memczak, M. Jens, A. Elefsinioti, et al., Circular RNAs are a large class of animal RNAs with regulatory potency, Nature 495 (7441) (2013) 333–338, https://doi.org/10.1038/nature11928.
[76] D.P. Bartel, MicroRNAs: target recognition and regulatory functions, Cell 136 (2) (2009) 215–233, https://doi.org/10.1016/j.cell.2009.01.002.
[77] W.J. Ni, X.M. Leng, Dynamic miRNA-mRNA paradigms: new faces of miRNAs, Biochem. Biophys. Rep. 4 (2015) 337–341, https://doi.org/10.1016/j.bbrep.2015.10.011.
[78] C.Y. Yu, H.C. Kuo, The emerging roles and functions of circular RNAs and their generation, J. Biomed. Sci. 26 (1) (2019) 29, https://doi.org/10.1186/s12929-019-0523-z.
[79] R.H. Krishnan, L. Sadu, R.L. Akshaya, et al., Circ_CUX1/miR-130b-5p/p300 axis for parathyroid hormone-stimulation of Runx2 activity in rat osteoblasts: a combined bioinformatic and experimental approach, Int. J. Biol. Macromol. S0141–8130 (22) (2022), https://doi.org/10.1016/j.ijbiomac.2022.11.176, 02735-0. Advance online publication.
[80] Y. Huang, S. Wan, M. Yang, et al., Circ_0067680 expedites the osteogenic differentiation of human bone marrow-derived mesenchymal stem cells through miR-4429/CTNNB1/Wnt/β-catenin pathway, Biol. Direct 16 (1) (2021) 16, https://doi.org/10.1186/s13062-021-00302-w.
[81] B. Yue, J. Wang, W. Ru, et al., The circular RNA circHUWE1 sponges the miR-29b-AKT3 Axis to regulate myoblast development, Mol. Ther. Nucleic Acids 19 (2020) 1086–1097, https://doi.org/10.1016/j.omtn.2019.12.039.
[82] H. Ji, X. Cui, Y. Yang, et al., CircRNA hsa_circ_0006215 promotes osteogenic differentiation of BMSCs and enhances osteogenesis-angiogenesis coupling by competitively binding to miR-942-5p and regulating RUNX2 and VEGF, Aging (Albany NY) 13 (7) (2021) 10275–10288, https://doi.org/10.18632/aging.202791. Epub 2021 Apr 4. PMID: 33819188; PMCID: PMC8064180.
[83] K. Zhao, Q. Zhao, Z. Guo, et al., Hsa_Circ_0001275: a potential novel diagnostic biomarker for postmenopausal osteoporosis, Cell. Physiol. Biochem. : int. J. Experiment. Cellul. Physiol. Biochem. Pharmacol. 46 (6) (2018) 2508–2516, https://doi.org/10.1159/000489657.
[84] Q. Yin, J. Wang, Q. Fu, et al., CircRUNX2 through has-miR-203 regulates RUNX2 to prevent osteoporosis, J. Cell Mol. Med. 22 (12) (2018) 6112–6121, https://doi.org/10.1111/jcmm.13888.